Effect of Boundary Conditions on Glazed Flat-Plate Solar Collector Performance Test Results

Tomas Matuska and Viacheslav Shemelin

Czech Technical University in Prague, Prague (Czech Republic)

Abstract

This analysis investigates the effect of performance test boundary conditions on the glazed flat-plate solar collector performance test results. The current test standard allows for some variations in boundary conditions, which can lead to differences in thermal performance characteristics. This article focuses on variations in collector tilt angle, average air speed, solar irradiance at the collector plane, and heat transfer fluid flow rate. A series of experimental thermal performance evaluations of a specific flat-plate solar collector was conducted using an indoor solar simulator, following the ISO 9806 test standard under various boundary conditions. It was observed that differences in collector tilt angle and wind speed resulted in variations in thermal performance test results, especially under high values of reduced temperature difference. However, irradiance and heat transfer fluid flow rate variations did not yield significant differences in thermal performance test results. Subsequently, an annual simulation analysis was performed using ScenoCalc simulation software under various constant mean operating temperatures and the climatic conditions of Stockholm, Würzburg, and Athens. The results demonstrated that differences in test boundary conditions under the current test standard would not cause considerable differences in solar system energy output simulation results for the most common solar thermal system applications (pool heating, solar domestic hot water systems, and space heating). Conversely, differences in test boundary conditions could lead to significant disparities in energy output simulation results for high-temperature solar thermal applications, such as process heat thermal systems.

Keywords: solar thermal system, solar collector testing, simulation analysis, boundary conditions

1. Introduction

To design a solar thermal system, it is essential to know the thermal performance parameters of the solar flat-plate collector used in the system. Typically, the minimum information required includes the efficiency curve characteristics (η_0, a_1, and a_2) and the reference area (the collector gross area according to the ISO 9806 standard ("ISO 9806:2017. Solar energy — Solar thermal collectors — Test methods.," 2017)). However, a challenge arises because the testing procedure for thermal performance parameters allows for some variations in experimental boundary conditions as per the current standard. Specifically, the standard for indoor testing of glazed flat-plate solar collectors (using a solar simulator) under steady-state conditions states:

- The collector tilt angle is unspecified but should be included in the test protocol.
- The average air speed parallel to the collector plane should be maintained at 3 m s^{-1} ± 1 m s^{-1}.
- The hemispherical solar irradiance at the collector plane should exceed 700 W m^{-2}.

As a result, the thermal performance characteristics of the thermal collector, tested according to the valid standard under different boundary conditions, may vary. For instance, Müller-Schöll and Frei (2000) presented a method for calculating the uncertainty of the performance characteristic curve's parameters obtained during the performance test evaluation. In their work, the authors stated that slight deviations in the test boundary conditions of the same solar collector among different laboratories cause differences in the thermal performance testing results. Reddy (2011), in his comprehensive work, investigated the modelling process for engineers and scientists in detail and concluded that the difference in performance between the modelled on-site and obtained in laboratory conditions could be caused by many reasons. One of them is the difference between boundary conditions on-site and during the laboratory measurement. Mathioulakis et al. (2012) investigated the sources of uncertainty in solar system simulation results and concluded that any deviation in the collector test method can introduce additional uncertainty components to the final simulation results. Later, Sowmy et al. (2017) experimentally demonstrated that differences in test boundary conditions contribute to variations in thermal performance results.

Selection and/or peer review under responsibility of Scientific Committee
10.18086/eurosun.2024.07.12 Available at http://proceedings.ises.org

This study aims to investigate the influence of boundary conditions under the valid standard ISO 9806 on the performance characteristics of glazed flat-plate solar collectors. Firstly, the reference boundary conditions and the investigated parameters were identified. Secondly, a series of experimental thermal performance tests were performed to investigate the effect of each investigated parameter individually. Then, the minimum and maximum possible thermal performance characteristic curve variants were derived. Finally, a simulation analysis was performed to understand the effect of the test boundary conditions on a glazed flat-plate solar collector's thermal performance.

2. Methodology

To investigate the effect of boundary conditions on the performance of glazed flat-plate solar collectors, the reference solar collector was experimentally tested to obtain its performance characteristics under different boundary conditions. An indoor solar simulator was utilised to perform a steady-state efficiency testing procedure, followed by a thermal performance evaluation conducted in accordance with the ISO 9806 standard. Fig. 1(a) demonstrates the solar simulator test loop, while Fig. 1(b) illustrates the analysed collector on the test stand during the experimental testing. Tab. 1 summarises the utilised sensor's type and their accuracy.

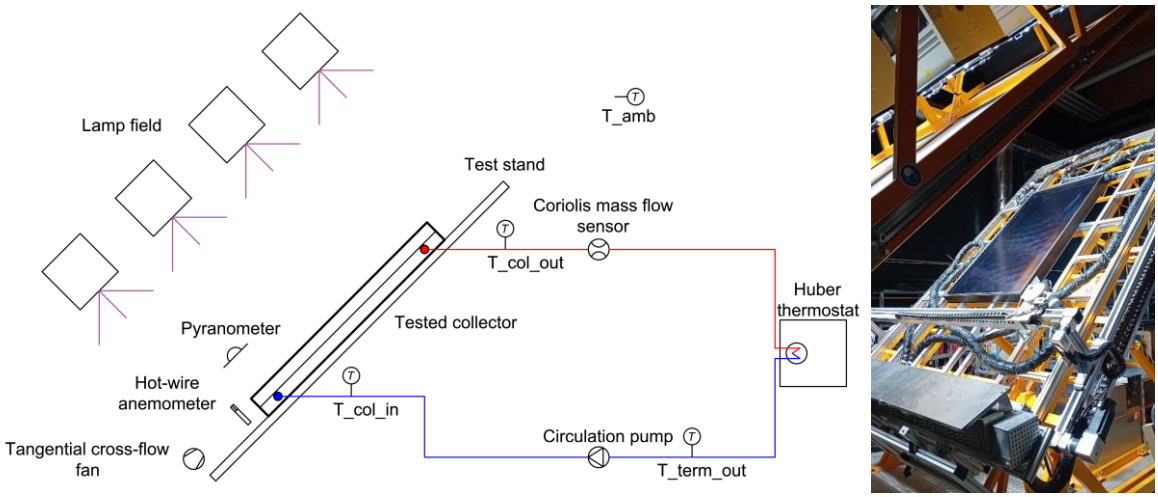

a) **b)**

Fig. 1: (a) The solar simulator test loop; (b) The analysed solar collector on the solar simulator test stand

Tab. 1: The sensors' type and their accuracy

Sensor	Manufacturer	Type	Accuracy
Temperature	TMG	PT100	± 0.05 K
Flow rate	Krohne	Coriolis mass flow sensor OPTIMASS 7000 T10	± 0.002%
Solar irradiation	Kipp & Zonen	Pyranometer SMP1 1 -A	± 1.4%
Wind velocity	Airflow Lufttechnik GmbH	Hot-wire anemometer D12-65V C	± 0.1 m/s

The effects of the following boundary conditions were analysed: collector tilt angle, solar irradiance at the collector plane, average air speed at the collector plane, and heat transfer fluid flow rate. The following conditions were considered as the reference boundary conditions for this investigation:

- Collector tilt angle of 45°,
- Hemispherical solar irradiance at the collector plane of 905 W m^{-2},
- Average air speed of 3 m s^{-1} at the collector plane,
- Heat transfer fluid flow rate of 72 kg m^{-2} h^{-1} of the collector gross area,
- Ambient air temperature of 18 °C.

It is worth noting that it is impossible to maintain the exact same values for the boundary condition parameters during the series of experimental tests. For instance, a solar irradiance homogeneity test was performed before each series of tests to ensure the homogeneity condition was fulfilled. Moreover, the average value of solar irradiance was determined for each test series during this test. Even though the lamps' position and power intensity were not changed, hemispherical solar irradiance at the collector plane may slightly differ (by a couple of watts). Therefore, the solar irradiance value, the heat transfer fluid flow rate value, and the ambient air temperature mentioned above are average values. Additionally, it should be emphasised that during all experimental tests, the actual values of these parameters did not vary by more than ±2% from the average values mentioned above.

To analyse the nature of the changes in the obtained thermal performance characteristics caused by different boundary conditions, a detailed validated model of a glazed flat-plate collector designed in TRNSYS simulation software was utilised (Shemelin and Matuska, 2017).

2.1. Effect of collector tilt angle

Firstly, the effect of the solar collector tilt angle was investigated. The reference setup conditions were applied, and the collector tilt angle was varied. The thermal performance evaluation was performed for seven tilt angles ranging from 0° to 90° with a 15° angle increment (see Fig. 2a). The results indicated a decrease in the thermal efficiency of the solar collector as the collector tilt angle decreased. This decline can be attributed to the increasing heat transfer by natural convection in the closed air gap between the absorber and the glazing. Increasing natural convection heat transfer significantly impacts the front-side heat loss and, consequently, the overall heat loss of the collector.

To confirm this, the heat transfer by convection in the closed gap between the absorber and the glazing was modelled using the detailed validated model of a glazed flat-plate collector. The obtained thermal resistance values of the convection heat transfer are plotted in Fig. 2b for various tilt angles (0°, 15°, 30°, …, 90°). The aim was to analyse the effect of the layer inclination angle on the natural convection heat transfer in the closed gap between the absorber and the glazing.

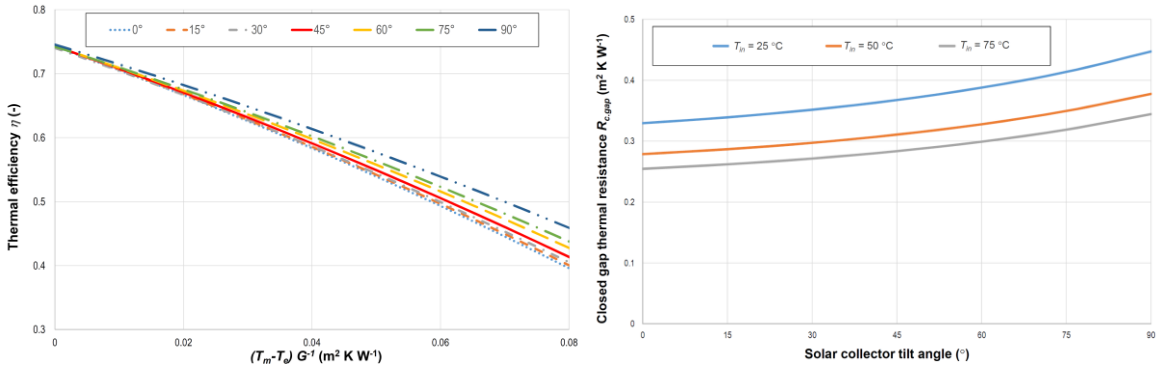

a) **b)**

Fig. 2: (a) The solar collector's thermal performance under different tilt angles; (b) The closed gap convection thermal resistance under different tilt angles and different mean operating temperatures

The results reveal a consistently increasing trend in the closed gap natural convection thermal resistance as the tilt angle of the collector increases. In the horizontal position, the thermal resistance is minimal, the heat transfer by convection is highest, and the solar collector has higher heat losses. In contrast, the vertical position minimises the heat losses (maximum thermal resistance); hence, the collector's thermal efficiency is higher. It can be noted that the thermal resistance through the air gap remains practically unchanged for low tilt angle values (0° to 30°). As a result, the efficiency curves are identical for collector inclinations ranging from 0° to 30°.

2.2. Effect of solar irradiance

Secondly, the effect of solar irradiance was analysed. The collector's thermal performance evaluation was performed for three solar irradiance levels. As mentioned before, the reference boundary condition for solar irradiance at the collector plane was 909 W m^{-2}. Then, the lamp positions were adjusted to increase solar irradiance at the collector plane to 1126 W m^{-2}. After that, the lamp field power was reduced by 14% (on

average) to decrease the solar irradiance to 827 W m^{-2}. It is worth noting that the irradiance homogeneity condition was fulfilled; the solar irradiance value at each measured point at the collector plane fell within a ±15% interval of the average irradiance at the collector plane. The obtained thermal performance characteristic curves under the different solar irradiance values are illustrated in Fig. 3. The figure indicates that there is no significant difference between the obtained thermal performance. Therefore, it is evident that the solar irradiance boundary condition specified in the test standard (the hemispherical solar irradiance at the collector plane should exceed 700 W m^{-2}) fully fulfils its purpose: following the standard leads to a specific solar collector performance result.

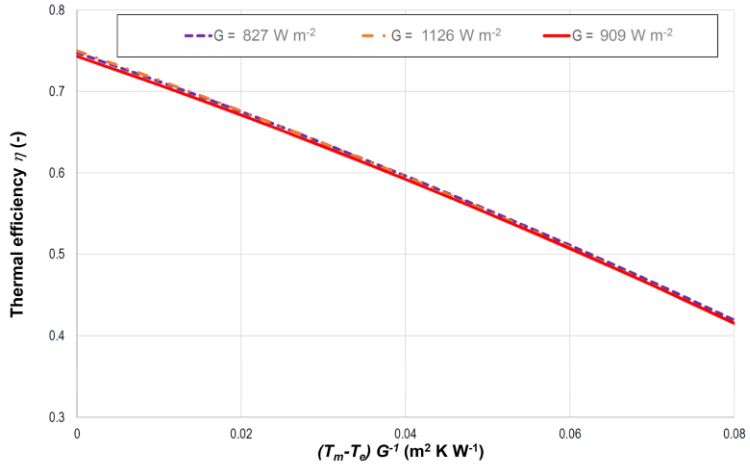

Fig. 3: The obtained thermal performance characteristic curves under different solar irradiances

2.3 Effect of wind speed

Thirdly, the effect of wind speed was investigated. The thermal efficiency evaluation based on the experimental test results was conducted for six wind speed velocities: 2 m s^{-1}, 3 m s^{-1}, and 4 m s^{-1} (according to the valid standard), as well as 0 m s^{-1}, 1.5 m s^{-1}, and 4.5 m s^{-1} to provide a complete understanding. The results of the evaluation are demonstrated in Fig. 4.

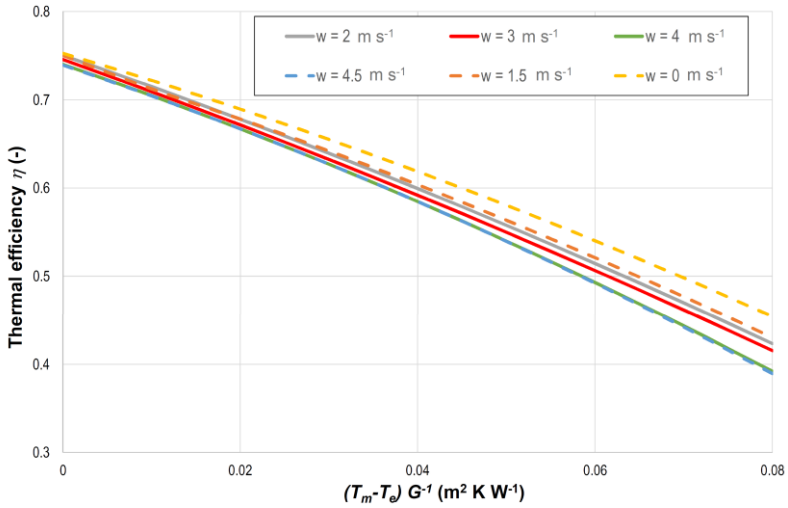

Fig. 4: The evaluated thermal performance characteristic curves under different wind speeds

The reference boundary conditions were applied, and only the artificial wind fan speed settings were changed to obtain different wind speeds. For the reference variant, the average wind speed at the collector plane was measured at 3 m s^{-1} (under 60% of fan power). The reduced and increased wind speed variants were achieved by decreasing and increasing fan power. Specifically, to achieve an average speed of 2 m s^{-1}, the fan's power was reduced to 43%; to achieve an average speed of 4 m s^{-1}, the power was increased to 86%. In addition, the performance evaluation procedure was also carried out for average wind speeds of 4.5 m s^{-1}, 1.5 m s^{-1}, and 0 m s^{-1}. Although these wind speeds no longer correspond to the current test conditions, the results can be helpful in analysing the effect of wind speed.

The effect of wind speed on the collector's thermal performance is significant for solar collectors with a high value of the collector front-side heat loss coefficient. The front-side heat loss coefficient depends on the closed-gap convection and thermal radiation between the absorber and the front-side glazing thermal resistances, the thermal resistance of the glazing itself, and the combined (wind and natural) convection and thermal radiation from the glazing's front-side thermal resistances. Therefore, to analyse the influence of wind speed on the collector's thermal performance, the combined convection thermal resistance has to be modelled. The problem is that more than 90 correlations can be applied to model the forced convection heat transfer coefficients (Palyvos, 2008). Around 35 of them, with some reservations, can be applied to model the forced convection heat transfer coefficients of a glazed flat plate collector (Shemelin and Matuška, 2023). Fig. 5a demonstrates the combined convection thermal resistance calculated using all of them, while Fig. 5b indicates the combined convection thermal resistance calculated using the most widely used correlations for solar collector performance modelling (Kumar et al., 1997; McAdams, 1954; Sharples and Charlesworth, 1998; Test et al., 1981; Wattmuff et al., 1977) together with the closed gap convection heat transfer resistance.

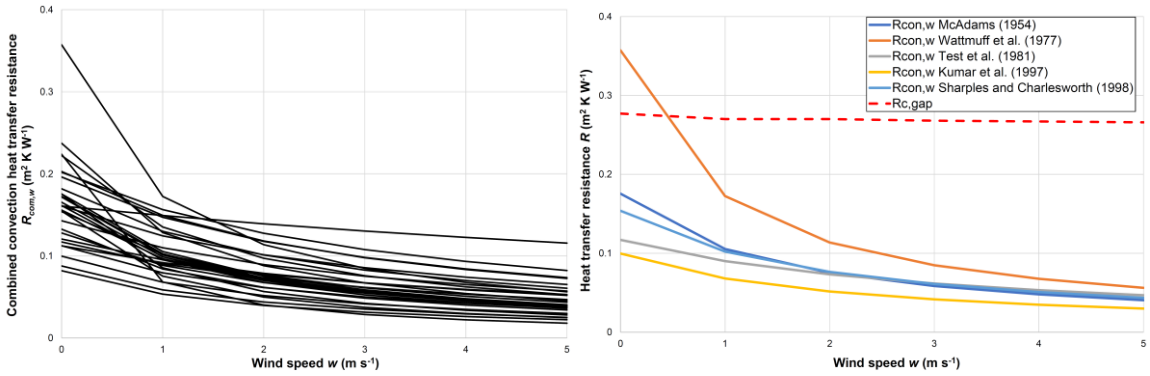

a) **b)**

Fig. 5: Combined convection heat transfer resistance calculated using (a) 35 correlations and (b) 5 widely used correlations in solar thermal modelling correlations

The modelling results indicated that under zero wind speed $w \rightarrow 0$ m s^{-1}, the combined convection heat transfer resistances reach their maximum values, and, more importantly, their values are comparable to the closed gap convection heat transfer resistance. As a result, it is evident that under such wind speeds, a solar collector's thermal performance also reaches its maximum. Under wind speeds in the range between 0 and 4 m s^{-1}, a decrease in thermal performance can be observed, caused by a decrease in the combined convection thermal resistance. The thermal efficiency remains the same under wind speeds higher than 4 m s^{-1}. This can be explained by the fact that changes in wind speed do not lead to significant changes in the combined convection heat transfer resistance at such speeds (see Fig. 5a). Moreover, these changes are insignificant considering the magnitude difference between the combined convection heat transfer resistance and the closed gap convection heat resistance (see Fig. 5b).

Therefore, the current standard sets the wind speed testing interval in the range between 2 and 4 m s^{-1}. Higher wind speeds do not significantly change thermal performance characteristic curves, while lower wind speeds do not adequately represent the on-site wind conditions. However, it is worth noting that even though there is no significant difference in thermal performance within the range between 2 and 4 m s^{-1} under low- and middle values of the reduced temperature difference, there is a considerable difference in thermal performance under high values of the reduced temperature difference.

2.4 Effect of heat transfer fluid flow rate

Moreover, the thermal performance efficiency test was also performed for three different values of the heat transfer fluid flow rates. The reference heat transfer fluid flow rate was 72 kg m^{-2} h^{-1}, while the reduced flow rate was 50% of the reference one, about 36 kg m^{-2} h^{-1}, and the increased flow rate was 150% of the reference flow rate, around 108 kg m^{-2} h^{-1}. The results of the testing are illustrated in Fig. 6.

Firstly, the tested variants with the reference and increased flow rates demonstrate similar thermal performance characteristic curves under the low value of the reduced temperature difference. Then, the increased flow rate variant showed higher thermal performance compared to the reference one. Finally, the reference variant demonstrated higher thermal performance compared to the increased flow rate variant under a relatively high

value of the reduced temperature difference. As for the reduced flow rate variant, it showed slightly lower thermal performance throughout the whole range of operating conditions. The Reynolds and average Nusselt numbers were further calculated using the detailed model to investigate this issue. The modelling results are illustrated in Fig. 7. It is worth noting that a considerable number of Nusselt number correlations describe the forced convection heat transfer process (Churchill and Ozoe, 1973; Colburn, 1964; Dittus and Boelter, 1985; Gnielinski, 1976; Hausen, 1943; Kakaç et al., 1987; Petukhov, 1970; Shah and London, 2014; Sieder and Tate, 1936; Sleicher and Rouse, 1975). As a result, the application of different equations leads to different results. In this work, the correlations initially presented by Shah (Shah and London, 2014) are utilised.

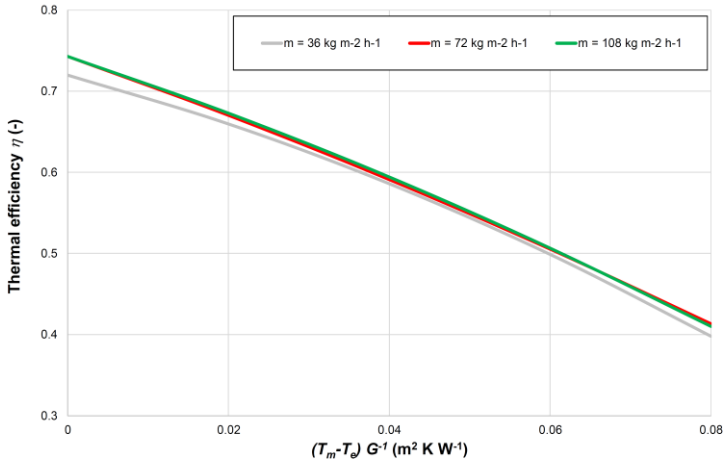

Fig. 6: The obtained thermal performance characteristic curves under different heat transfer fluid flow rates

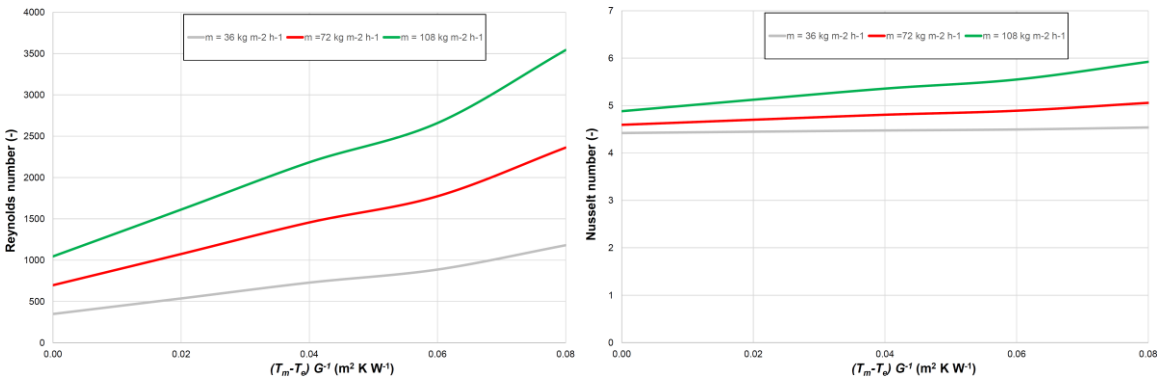

a) **b)**

Fig. 7: (a) Reynolds and (b) Nusselt number modelling results under considered operating conditions

These results show that under the considered operating conditions, the heat transfer fluid flow is primarily laminar (*Re* < 2300). For a few measured points, the flow proceeds to the transition zone between laminar and turbulent flow, where it is impossible to identify precisely whether it is laminar or turbulent. Considering these facts, the forced convection heat transfer correlations (for the fully developed flow and entrance region) initially presented by Shah were applied for calculation purposes (Shah and London, 2014). According to the calculation results, the reference variant and the increased flow rate variant outperform the reduced flow rate variant over the entire measured range. The higher Nusselt numbers eventually lead to a higher value of the forced convection heat transfer coefficient, resulting in higher energy performance. The modelling results, utilising the detailed validated flat-plate collector model, confirm this. Therefore, it can be concluded that inconsistent results during this series of experiments can be attributed to the measurement uncertainty caused by sensors' accuracy and the repeatability of readout values. Since the difference in thermal performance between analysed variants is minor, the measurement uncertainty can mix up with the results. Thus, it was decided not to include the flow rate parameter in the simulation analysis presented in the next chapter.

3. Simulation analysis

The experimental testing results mentioned above demonstrated that the collector tilt angle and wind speed considerably affect the tested collector's thermal performance. The thermal performance increases with increasing slope and decreasing wind speeds. According to the current standard, the maximum possible thermal efficiency will be the thermal characteristic curve obtained under a wind speed of 2 m s^{-1} and a collector's tilt angle of 0 degrees (variant MAX). Conversely, the minimum possible thermal efficiency will be the thermal characteristic curve obtained under a wind speed of 4 m s^{-1} and a collector's tilt angle of 90 degrees (variant MIN). These two variants were obtained using the experimental and simulation results from the detailed validated mathematical model. The thermal performance characteristic curve derived under the reference boundary conditions, with a wind speed of 4 m s^{-1} and a collector's tilt angle of 90 degrees, was selected as the reference variant RV. The efficiency characteristic curves of the compared variants are shown in Fig. 8.

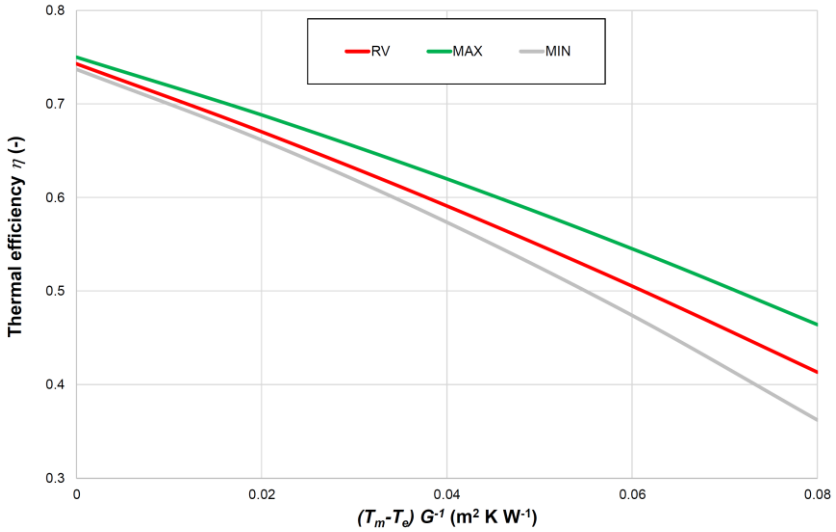

Fig. 8: The analysed thermal performance variants

The simulation analysis should be performed to understand the effect of the test boundary conditions on a glazed flat-plate solar collector's thermal performance. While the individual thermal performance characteristic curves demonstrate the variation in thermal performance under different boundary conditions, this is not a telling comparison because the collector's operating point moves along part of the presented efficiency curve in ordinary operation. Furthermore, the collector's heat transfer fluid operating temperature defines the operating region. Therefore, it was decided to perform a simulation analysis for different operating temperatures using ScenoCalc software.

To obtain a comprehensive understanding of the influence of boundary conditions on the performance results and, consequently, the solar system's performance simulation results, an annual simulation analysis was performed using ScenoCalc simulation software. This software allows the calculation of an annual solar collector's energy output using the obtained thermal performance characteristic curves under constant operating temperatures and different climatic conditions. To represent different solar collector applications, ranging from pool heating to process heat, the following constant collector mean operating temperatures were applied: 25 °C, 50 °C, 75 °C, and 100 °C. Moreover, to represent different climatic zones, the climatic conditions of Stockholm (Sweden), Würzburg (Germany), and Athens (Greece) were considered.

4. Results and discussion

The simulation results for the considered collector variants (MAX, MIN, and RV) under different operating temperatures and climatic conditions are presented in

Tab. 2. Additionally, the results for Stockholm and Athens climatic conditions are illustrated in Fig. 9.

The simulation results indicated that below the operating temperature of 50 °C, the difference between the simulated variants is not significant for all climatic conditions. Specifically, the annual solar collector's energy output varies between -5% and 10% if the reference boundary conditions are not met during the performance

evaluation test. In contrast, the simulation results demonstrated that for operating temperatures higher than 50 °C, the difference between the annual solar collector's energy output becomes significant. For instance, under the operating temperature of 100 °C and the climatic conditions of Würzburg, the simulated annual solar collector's energy output varies between -25% and +29%. The situation is also similar for the other climatic conditions.

Tab. 2: Simulation results under various operating temperatures and climate conditions

	Annual solar collector's energy output (kWh m^{-2})			
	25 °C	**50 °C**	**75 °C**	**100 °C**
Stockholm (Sweden), incident solar irradiation 1166 kWh m^{-2} (yearly)				
MIN	635 (-2%)	407 (-5%)	237 (-12%)	113 (-27%)
RV	645	429	271	154
MAX	670 (+4%)	472 (+10%)	319 (+18%)	201 (+30%)
Würzburg (Germany), incident solar irradiation 1228 kWh m^{-2} (yearly)				
MIN	685 (-1%)	435 (-5%)	250 (-13%)	122 (-25%)
RV	695	458	286	163
MAX	720 (+4%)	505 (+10%)	338 (+18%)	209 (+29%)
Athens (Greece), incident solar irradiation 1170 kWh m^{-2} (yearly)				
MIN	1109 (-1%)	773 (-3%)	487 (-9%)	251 (-22%)
RV	1121	799	537	319
MAX	1138 (+2%)	857 (+7%)	612 (+14%)	402 (+26%)

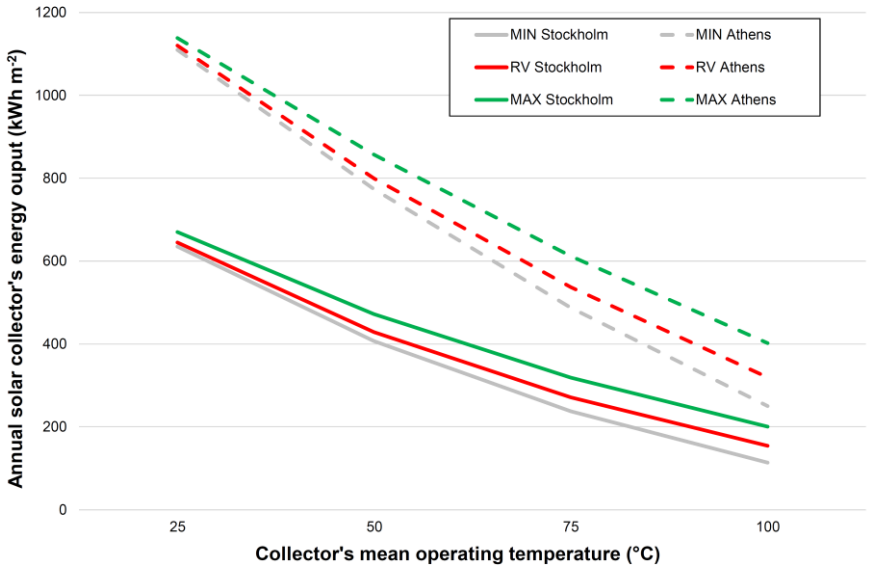

Fig. 9: Annual solar collector's simulation results under different operating and climatic conditions

To sum up, differences in test boundary conditions (under the valid standard) are unlikely to cause any considerable difference in the simulated annual solar collector's energy output during the design stage for systems such as solar pool heating systems or solar domestic hot water systems. In contrast, the annual solar collector's energy output difference is much more significant under the collector's mean temperature between 50 °C and 100 °C. Thus, for such systems (for instance, solar process heat systems), it is highly recommended that the boundary conditions under which the performance test was carried out be considered before performing the simulation analysis at the design stage. In any case, it is essential to emphasise that for such systems (with high operating temperatures), the differences in test boundary conditions will cause significant uncertainty in the energy simulation results.

5. Conclusion

This paper investigated the effect of boundary conditions on the performance evaluation test results of glazed flat-plate collectors. Firstly, the reference boundary conditions and the investigated parameters were identified. Secondly, a series of experimental thermal performance tests were performed to investigate the effect of each parameter individually. Then, the minimum and maximum possible thermal performance characteristic curves were derived. Finally, a simulation analysis was performed to understand the effect of the test boundary conditions on a glazed flat-plate solar collector's thermal performance. The following conclusions can be made:

- The experimental results demonstrated a negligible effect of solar irradiance and the heat transfer fluid flow rate (under the valid standard) on the solar collector's thermal performance.
- In contrast, wind speed and collector tilt angle during the performance evaluation test considerably affect the obtained thermal performance characteristic curves.
- The results showed that the difference in the test boundary conditions under the valid test standard would not cause any considerable difference in the solar system energy output simulation results performed at the design stage for the most common solar thermal system applications (pool heating, solar domestic hot water systems, and space heating).
- Conversely, the differences in test boundary conditions could lead to significant disparities in energy output simulation results for high-temperature solar thermal applications, such as process heat.

6. References

Churchill, S.W., Ozoe, H., 1973. Correlations for laminar forced convection in flow over an isothermal flat plate and in developing and fully developed flow in an isothermal tube. J. Heat Transfer 95, 416–419.

Colburn, A.P., 1964. A method of correlating forced convection heat-transfer data and a comparison with fluid friction. Int. J. Heat Mass Transf. 7, 1359–1384.

Dittus, F.W., Boelter, L.M.K., 1985. Heat transfer in automobile radiators of the tubular type. Int. Commun. Heat Mass Transf. 12, 3–22.

Gnielinski, V., 1976. New equations for heat and mass transfer in turbulent pipe and channel flow. Int. Chem. Eng. 16, 359–368.

Hausen, H., 1943. Darstellung des Warmeuberganges in Rohren durch verallgemeinerte Potenzbeziehungen. Z. VDI Beih. Verfahrenstech 4, 91–98.

ISO 9806:2017. Solar energy — Solar thermal collectors — Test methods., 2017.

Kakaç, S., Shah, R.K., Aung, W., others, 1987. Handbook of single-phase convective heat transfer. Wiley New York et al.

Kumar, S., Sharma, V.B., Kandpal, T.C., Mullick, S.C., 1997. Wind induced heat losses from outer cover of solar collectors. Renew. Energy 10, 613–616. https://doi.org/10.1016/S0960-1481(96)00031-6

Mathioulakis, E., Panaras, G., Belessiotis, V., 2012. Uncertainty in estimating the performance of solar thermal systems. Sol. Energy 86, 3450–3459. https://doi.org/10.1016/j.solener.2012.07.025

McAdams, W.H., 1954. Heat Transmission 3d Ed. McGraw-Hill, New York.

Müller-Schöll, C., Frei, U., 2000. Uncertainty analyses in solar collector measurement, in: Proceedings of the Eurosun Congress. Copenhagen, Denmark.

Palyvos, J.A., 2008. A survey of wind convection coefficient correlations for building envelope energy systems' modeling. Appl. Therm. Eng. 28, 801–808. https://doi.org/10.1016/j.applthermaleng.2007.12.005

Petukhov, B.S., 1970. Heat transfer and friction in turbulent pipe flow with variable physical properties. Adv. heat Transf. 6, 503–564.

Reddy, T.A., 2011. Applied Data Analysis and Modeling for Energy Engineers and Scientists. Springer US, Boston, MA. https://doi.org/10.1007/978-1-4419-9613-8

Shah, R.K., London, A.L., 2014. Laminar flow forced convection in ducts: a source book for compact heat exchanger analytical data. Academic press.

Sharples, S., Charlesworth, P.S., 1998. Full-scale measurements of wind-induced convective heat transfer

from a roof-mounted flat plate solar collector. Sol. Energy 62, 69–77.

Shemelin, V., Matuska, T., 2017. Detailed Modeling of Flat Plate Solar Collector with Vacuum Glazing. Int. J. Photoenergy 2017, 1–9. https://doi.org/10.1155/2017/1587592

Shemelin, V., Matuška, T., 2023. The effect of the wind conditions on the thermal performance of an unglazed solar thermal collector. Energy Reports 10, 2880–2888. https://doi.org/10.1016/j.egyr.2023.09.132

Sieder, E.N., Tate, G.E., 1936. Heat Transfer and Pressure Drop of Liquids in Tubes. Ind. Eng. Chem. 28, 1429–1435. https://doi.org/10.1021/ie50324a027

Sleicher, C., Rouse, M.W., 1975. A convenient correlation for heat transfer to constant and variable property fluids in turbulent pipe flow. Int. J. Heat Mass Transf. 18, 677–683.

Sowmy, D.S., Schiavon Ara, P.J., Prado, R.T.A., 2017. Uncertainties associated with solar collector efficiency test using an artificial solar simulator. Renew. Energy 108, 644–651. https://doi.org/10.1016/j.renene.2016.08.054

Test, F.L., Lessmann, R.C., Johary, A., 1981. Heat Transfer During Wind Flow over Rectangular Bodies in the Natural Environment. J. Heat Transfer 103, 262–267.

Wattmuff, J.H., Charters, W.W.S., Proctor, D., 1977. Solar and wind induced external coefficients for solar collectors. Coop. Mediterr. pour l'Energie Solaire, Rev. Int. d'Heliotechnique 2, 56.